



# 1 Development and Validation of a New In-Situ Technique 2 to Measure Total Gaseous Chlorine in Ambient Air

3

4 Teles C. Furlani<sup>1</sup>, Peter M. Edwards<sup>2</sup>, Tara F. Kahan<sup>3</sup>, Cora J. Young<sup>1\*</sup>

5 <sup>1</sup> Department of Chemistry, York University, Toronto, Canada

6 <sup>2</sup> Department of Chemistry, University of York, York, UK

7 <sup>3</sup> Department of Chemistry, University of Saskatchewan, Saskatoon, Canada

8

9 \*Correspondence to: youngcj@yorku.ca

10

## 11 **Abstract**

12 Total gaseous chlorine (TCl<sub>g</sub>) measurements can improve our understanding of unknown sources  
13 of Cl to the atmosphere. Existing techniques for measuring TCl<sub>g</sub> have been limited to offline  
14 analysis of extracted filters and do not provide suitable temporal information on fast atmospheric  
15 process. We describe high time-resolution in-situ measurements of TCl<sub>g</sub> by combusting ambient  
16 air over a heated platinum (Pt) substrate coupled to a cavity ring-down spectrometer (CRDS).  
17 The method relies on the complete decomposition of TCl<sub>g</sub> to release Cl atoms that react to form  
18 HCl, for which detection by CRDS has been shown to be fast and reliable. The method was  
19 validated using custom organochlorine permeation devices (PDs) that generated gas-phase  
20 dichloromethane (DCM), 1-chlorobutane (CB), and 1,3-dichloropropene (DCP). The optimal  
21 conversion temperature and residence time through the high-temperature furnace was 825 °C and  
22 1.5 seconds, respectively. Complete conversion was indicated by the near unity orthogonal  
23 distance regression analysis slope ( $\pm\sigma$ ) of  $0.996 \pm 0.012$ ,  $1.048 \pm 0.006$ , and  $1.027 \pm 0.061$  for  
24 DCM, CB, and DCP, respectively. Breaking these strong C-Cl bonds represents a proof of  
25 concept for complete conversion of all similar or weaker bonds that characterize all other TCl<sub>g</sub>.



26 We applied this technique to both outdoor and indoor environments and found reasonable  
27 comparisons in ambient background mixing ratios with the sum of expected HCl from known Cl  
28 species. We measured the converted  $\text{TCl}_g$  in an indoor environment during cleaning activities  
29 and observed varying levels of  $\text{TCl}_g$  comparable to previous studies. The method validated here  
30 is capable of measuring in-situ  $\text{TCl}_g$  and has a broad range of applications to make routine  $\text{TCl}_g$   
31 measurements in a variety of applications.

## 32 **1. Introduction**

33 Chlorine (Cl) containing compounds in the atmosphere can impact air quality, climate,  
34 and health (Massin et al., 1998; Saiz-Lopez and Von Glasow, 2012; Simpson et al., 2015; White  
35 and Martin, 2010). Gaseous chlorinated compounds are either organic (e.g., dichloromethane,  
36 chloroform, and carbon tetrachloride) or inorganic (e.g.,  $\text{Cl}_2$ , HCl, and  $\text{ClNO}_2$ ), with inorganic  
37 chlorine being more reactive under most atmospheric conditions. In this work, total gaseous  
38 chlorine ( $\text{TCl}_g$ ) refers to all gas-phase chlorine-containing species, including both inorganic and  
39 organic species. Impacts on air quality and climate are due to the high reactivity of atomic Cl  
40 produced by common atmospheric reactions (e.g., photolysis and oxidation) of Cl-containing  
41 compounds (Haskins et al., 2018; Riedel et al., 2014; Sherwen et al., 2016). The Cl cycle is  
42 important to atmospheric composition in the stratosphere and troposphere, affecting species  
43 including methane, ozone, and particles (both formation and composition), which influence air  
44 quality and climate (Riedel et al., 2014; Sherwen et al., 2016; Solomon, 1999; Young et al.,  
45 2014). High levels of some  $\text{TCl}_g$  species (e.g.,  $\text{Cl}_2$  and carbon tetrachloride) are known to be  
46 toxic (Unsal et al., 2021; White and Martin, 2010). The implications of many  $\text{TCl}_g$  species on  
47 human health are not well understood for low level exposure for extended periods of time.  
48 Potential health impacts of organic chlorinated compounds include hepatotoxicity,



49 nephrotoxicity, and genotoxicity (Henschler, 1994; Unsal et al., 2021). Impacts of inorganic  
50 chlorinated species include the chlorination of squalene, a major part of human skin oils, by  
51 HOCl (Schwartz-Narbonne et al., 2019); respiratory irritation and airway obstruction by Cl<sub>2</sub>  
52 (White and Martin, 2010); and increased incidence of asthma and other chronic respiratory issues  
53 following exposure to chloramines (Massin et al., 1998).

54 Sources of Cl to the atmosphere are highly variable and depend on both direct emissions  
55 and indirect regional Cl activation chemistry (Finlayson-Pitts, 1993; Khalil et al., 1999; Raff et  
56 al., 2009). Direct emissions of TCl<sub>g</sub> can come from numerous natural and anthropogenic  
57 activities such as, but not limited to, ocean and volcanic emissions, biomass burning, disinfection  
58 (i.e., household cleaning, pool emission, etc), use of solvents and heat transfer coolants, and  
59 incineration of chlorinated wastes (Blankenship et al., 1994; Butz et al., 2017; Fernando et al.,  
60 2014; Keene et al., 1999; Lobert et al., 1999; Wong et al., 2017). Activation of Cl is another  
61 source, occurring when atmospheric processes transform relatively unreactive chloride (Cl<sup>-</sup>) into  
62 reactive gaseous chlorine (Cl<sub>y</sub>), which will contribute to TCl<sub>g</sub>. Understanding global levels of  
63 TCl<sub>g</sub> is difficult due to complex emissions and chemistry. Our best estimates come from  
64 modelling studies combined with collaborative efforts to compose policy reports on halogenated  
65 substances, such as the World Meteorological Organization (WMO) Scientific Assessment of  
66 Stratospheric Ozone Depletion (WMO, 2018). Mixing ratio estimates of halogenated species  
67 from this report are summed from individual measurements (e.g., National Oceanic and  
68 Atmospheric Administration (NOAA) and Advanced Global Atmospheric Gases Experiment  
69 (AGAGE)). The WMO report includes flask (captured gas from clean air sectors) and in-situ  
70 measurements from field campaigns and routine sampling sites (e.g., CONvective Transport of  
71 Active Species in the Tropics (CONTRAST)) (Adcock et al., 2018; Andrews et al., 2016;



72 Montzka et al., 2021; Pan et al., 2017; Prinn et al., 2018). In the most recent WMO report  
73 (WMO, 2018), a decrease of  $12.7 \pm 0.9$  pptv  $\text{Cl yr}^{-1}$  in total tropospheric Cl was determined for  
74 Montreal Protocol-controlled substances (e.g., chlorofluorocarbons (CFCs) and  
75 hydrochlorofluorocarbons (HCFCs)). The decrease in Montreal Protocol-controlled emissions  
76 has been slightly offset by an increase in relatively short-lived substances (e.g., dichloromethane)  
77 that are not controlled by the Montreal Protocol (WMO, 2018). Despite the emissions of these  
78 regulated chlorinated species being relatively well-constrained, new sources for some of these  
79 compounds have appeared in the recent past. For example, unexpected increases observed in  
80 CFC-11 emissions suggested new unreported production (WMO, 2018). A new source of  
81 chloroform was also recently identified and attributed to halide containing organic matter derived  
82 from penguin excrement in the Antarctic tundra (Zhang et al., 2021). Atmospheric levels of  $\text{TCI}_g$   
83 will additionally be impacted by emission sources that are relatively poorly constrained,  
84 including combustion and disinfection. Increasing levels of chlorinated species from known and  
85 unknown pathways was observed in a recent ice core study, which estimated an increase of up to  
86 170% of  $\text{Cl}_y$  ( $= \text{BrCl} + \text{HCl} + \text{Cl} + \text{ClO} + \text{HOCl} + \text{ClNO}_3 + \text{ClNO}_2 + \text{ClOO} + \text{OCIO} + 2\cdot\text{Cl}_2 +$   
87  $2\cdot\text{Cl}_2\text{O}_2 + \text{ICl}$ ) from preindustrial times to the 1970s could be attributed to mostly anthropogenic  
88 sources (Zhai et al., 2021).

89         Understanding  $\text{TCI}_g$  source and sink chemistry is not only important for the ambient  
90 atmosphere but also for indoor environments. Uncertainty in sources and levels of chemicals,  
91 including chlorine-containing compounds, indoors is related to heterogeneity in sources and  
92 individual indoor environments, and the fact that relatively few studies have focused on indoor  
93 chemistry compared to outdoor. The role of chlorinated species on indoor air quality has been  
94 investigated in a few studies (Dawe et al., 2019; Doucette et al., 2018; Giardino and Andelman,

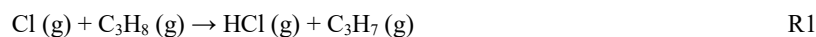


95 1996; Mattila et al., 2020; Nuckols et al., 2005; Shepherd et al., 1996; Wong et al., 2017). Most  
96 studies have focused on cleaning with chlorine-based cleaners, in which HOCl and other  
97 inorganic compounds have been observed in the gas phase at high levels (Mattila et al., 2020;  
98 Wang et al., 2019; Wong et al., 2017). Some studies have reported the presence of organic  
99 chlorinated species such as chloroform and carbon tetrachloride above bleach cleaning solutions  
100 indoors (Odabasi, 2008; Odabasi et al., 2014), and chloroform has been observed during water-  
101 based cleaning activities, such as showering and clothing washing (Giardino and Andelman,  
102 1996; Nuckols et al., 2005; Shepherd et al., 1996).

103         Constraining the Cl budget is critical to better understanding its contributions to climate,  
104 air quality, and human health. Robust total Cl measurements are useful because it is not feasible  
105 to routinely deploy individual measurements of the large number of Cl-containing compounds  
106 (Table S1). As described above, estimates of  $\text{TCI}_g$  from models and summed measurements have  
107 demonstrated gaps in our knowledge. It is therefore essential to have a method capable of  
108 measuring true  $\text{TCI}_g$  to explain discrepancies between model and measured estimates due to  
109 unknown species. Measurements of total elemental composition in the condensed phase,  
110 including total Cl, have been used for monitoring and managing both known and unknown  
111 compounds (Kannan et al., 1999; Kawano et al., 2007; Miyake et al., 2007c, 2007a, 2007b; Xu et  
112 al., 2003; Yeung et al., 2008). However,  $\text{TCI}_g$  methods have been limited to offline analysis of  
113 scrubbed sample gas (e.g., flue); these methods rely on multiple extraction steps and the  
114 application of condensed-phase total Cl analyses, such as combustion ion chromatography (Kato  
115 et al., 2000; Miyake et al., 2007a) or neutron activation analysis (Berg et al., 1980; Xu et al.,  
116 2006, 2007). Because offline techniques suffer from extraction uncertainties and do not have the  
117 temporal resolution to effectively probe fast source and sink chemistry in the atmosphere, in-situ



118 measurements of total elemental gaseous composition have been developed for several elements  
119 (Hardy and Knarr, 1982; Maris et al., 2003; Roberts et al., 1998; Veres et al., 2010). For  
120 example, total nitrogen has been measured using Pt-catalyzed thermolysis coupled to online  
121 chemiluminescence detection (Stockwell et al., 2018). Using a similar approach, we describe  
122 here a method for  $\text{TCl}_g$ , where catalyzed thermolysis is coupled to a high time-resolution HCl  
123 cavity ring-down spectrometer (CRDS). This technique relies on the complete thermolysis of  
124  $\text{TCl}_g$ , which yields chlorine atoms. These Cl atoms readily form HCl via hydrogen abstraction  
125 (R1), in this case from propane that is supplied in excess.



126 The objectives of this paper are to: (i) Develop and validate an instrument capable of in-  
127 situ measurement of  $\text{TCl}_g$  through conversion to HCl and detection by CRDS; and (ii)  
128 demonstrate application of the technique to outdoor and indoor  $\text{TCl}_g$  measurements.

## 129 **2. Materials and experimental methods**

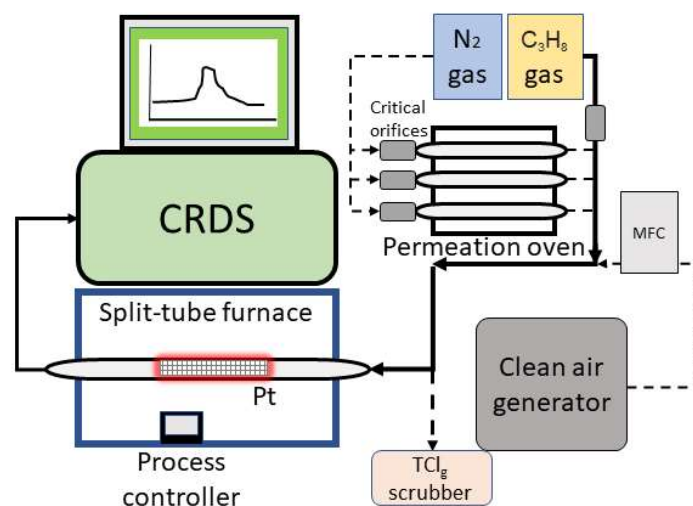
### 130 **2.1. Chemicals**

131 Commercially available reagents were purchased from Sigma-Aldrich: dichloromethane  
132 (DCM, HPLC grade, Oakville, Ontario, Canada), 1-chlorobutane (CB, 99.5%, Milwaukee,  
133 Wisconsin, USA), cis-1,3-dichloropropene (DCP, 97%, Milwaukee, Wisconsin, USA), and 52  
134 mesh sized platinum catalyst (99.9 %, Milwaukee, Wisconsin, USA). Nitrogen (grade 4.8) and  
135 propane ( $\text{C}_3\text{H}_8$ , 12.7% in nitrogen, v/v) gas was from Praxair (Toronto, Ontario, Canada).  
136 Experiments used deionized water generated by a Barnstead Infinity Ultrapure Water System  
137 (Thermo Fisher Scientific, Waltham, Massachusetts, USA;  $18.2 \text{ M}\Omega \text{ cm}^{-1}$ ). Clean air was  
138 generated by a custom-made zero-air generator.



139 **2.2. HCl and total chlorine (HCl-TCl) instrument**

140 The main components of the HCl-TCl (Figure 1) are platinum catalyst mesh, a quartz glass  
141 flow tube, a split-tube furnace (Protégé Compact, 1100°C max temperature, Thermcraft  
142 incorporated, North Carolina, USA), and a CRDS HCl analyzer (Picarro G2108 Hydrogen  
143 Chloride Gas Analyzer). The platinum catalyst consisted of ~2 g platinum mesh with a total  
144 combined surface area of 134 cm<sup>2</sup>. Sample gas was mixed with critical orifice-regulated (Lenox  
145 laser, Glen Arm, Maryland, USA, 30 psi; SS-4-VCR-2-50) propane gas (62 ± 6 standard cubic  
146 centimetres per minute (sccm)), provided in excess prior to introduction to the furnace to  
147 promote (R1). Propane does not fully combust at temperatures < 650 °C, which can lead to  
148 spectral interferences in the CRDS analyzer (Figure S1) and should only be added when  
149 temperatures exceed 650°C (Furlani et al., 2021). All lines and fittings were made of  
150 perfluoroalkoxy (PFA) unless stated otherwise. The mixing line carrying clean air dilution flows  
151 was controlled by a 10 L min<sup>-1</sup> mass flow controller (MFC, GM50A, MKS instruments,  
152 Andover, Massachusetts, USA). The length of the sample gas tubing to the furnace was 0.6 m,  
153 and the transfer line between the furnace and CRDS was 0.2 m. The coupled CRDS can capture  
154 transient fast HCl formation processes on the timescale of a few minutes, limited by inlet effects.  
155 The CRDS collects data at 0.5 Hz, which was averaged to 30 sec for the purposes of this work.  
156 LODs were calculated as three times the Allan–Werle deviation in raw signal intensity when  
157 overflowing the inlet with zero air directed into the CRDS for ~ 10 h. The 30-sec limit of  
158 detection (LOD) is 18 pptv and well below expected HCl from TCl<sub>g</sub> conversion (Furlani et al.,  
159 2021).



160

161 **Figure 1.** Sampling schematic showing the key components of the HCl-TCl coupled to the  
162 CRDS analyzer. Dashed lines indicate parts of the apparatus used only during validation. Not to  
163 scale.

### 164 2.3. Preparation of permeation devices (PDs)

165 Permeation devices (PDs) were prepared as follows: approximately 200  $\mu\text{L}$  of DCM, CB,  
166 or DCP was pipetted into a 50 mm PFA tube (3 mm i.d. with 1 mm thickness), thermally sealed  
167 at one end and plugged at the other end with porous polytetrafluoroethylene (PTFE) (13 mm  
168 length by 3.17 mm o.d.). The polymers allow a consistent mass of standard gas to permeate at a  
169 given temperature and pressure. The method for temperature and flow control of the PDs is  
170 described in detail in Lao et al. (2020). Briefly, an aluminum block that was temperature-  
171 controlled (Omega<sup>TM</sup>; CN 7823, Saint-Eustache, QC, Canada) using a cartridge heater  
172 (Omega<sup>TM</sup>; CIR-2081/120V, Saint-Eustache, QC, Canada) housed the PD and was regulated to  
173  $30.0 \pm 0.1$  °C. Dry  $\text{N}_2$  gas flowed through a PFA housing tube (1.27 cm o.d.) in the block that  
174 contained the PD. Stable flows of carrier gases passed through the housing tube in the oven were  
175 achieved using a 50  $\mu\text{m}$  diameter critical orifice (Lenox laser, Glen Arm, Maryland, USA, 30  
176 psi; SS-4-VCR-2-50) and were  $120 \pm 12$ ,  $99 \pm 9.9$  and  $120 \pm 12$  sccm for DCM, CB, and DCP,





177 respectively. Flows were measured using a DryCal Definer 220 (Mesa Labs, Lakewood,  
178 Colorado, USA). The mass emission rate of each organochlorine from the PDs was quantified  
179 gravimetrically over a period of approximately 4 weeks (mass accuracy  $\pm 0.001$  g). Mass  
180 emission rates for each PD were determined as  $640 \pm 10$ ,  $240 \pm 40$ , and  $1.20 \times 10^4 \pm 0.02 \times 10^4$  ng  
181  $\text{min}^{-1}$  ( $n=3$ ,  $\pm 1\sigma$ ) at  $30^\circ\text{C}$  for DCM, CB, and DCP, respectively.

#### 182 **2.4. HCl-TCl optimization**

183 Gas phase standards of DCM, CB, and DCP were used to test the conversion efficiency of  
184 chlorinated compounds to form HCl. Bond dissociation energies for carbon-Cl bonds typically  
185 range between  $310$  and  $410$   $\text{kJ mol}^{-1}$  (Tables S1, S2). The split-tube furnace has a process  
186 controller capable of increasing or decreasing temperature at a set  $^\circ\text{C min}^{-1}$ , which allowed us to  
187 identify the temperature at which enough energy was provided to break the bonds. By  
188 introducing a consistent amount of each of the organochlorines, separately, to the HCl-TCl set  
189 over a simple temperature ramping program we could monitor in real-time the conditions  
190 necessary to break the bonds by measuring the formation of the resulting HCl. The conversion  
191 temperature was determined when the measured HCl plateaued at 100% conversion.

192 To determine the optimal residence time in the quartz tube with the Pt catalyst, flows of  
193  $0.6\text{--}5.5$   $\text{L min}^{-1}$  containing DCM sample gas in clean air were tested yielding a range of  
194 residence times between  $0.5$  and  $4.5$  sec in the furnace. Temperature remained constant at  $825^\circ\text{C}$   
195 throughout the experiment, and a dilution flow of  $4.0$   $\text{L min}^{-1}$  of clean air was added to the  
196 sample flow exiting the furnace before introduction to the CRDS.

197 We tested the HCl-TCl conversion efficiency for 5 different mixing ratios of three  
198 organochlorine PD standards (DCM, CB, and DCP) under three conditions: (1) both Pt catalyst  
199 and added propane, (2) only Pt catalyst, and (3) only added propane. Each gas was tested



200 individually under the same conditions; sample gas from PDs was mixed with propane and  
201 immediately diluted into clean air using a 10 L min<sup>-1</sup> MFC (GM50A, MKS instruments,  
202 Andover, Massachusetts, USA). The dilution flows ranged from 2.2–9.0 L min<sup>-1</sup>. The sampling  
203 lines were the same lengths as stated previously. In this experiment, the CRDS flowrate of 2 L  
204 min<sup>-1</sup> was sufficient to give an optimal residence time of 1.5 sec through the HCl-TCl (see  
205 Section 3.1). In all experiments the CRDS subsampled through the furnace from the main  
206 transfer line and the excess gas was directed outdoors through a waste line containing a carbon  
207 trap (Purakol, Purafil, Inc, Doraville, Georgia, USA).

## 208 **2.5. Outdoor air HCl-TCl measurements**

209 Outdoor air sampling was performed on August 6 and November 17–19, 2021 (Eastern  
210 daylight time, EDT). The sampling site was the air quality research station located on the roof of  
211 the Petrie Science and Engineering building at York University in Toronto, Ontario, Canada  
212 (43.7738° N, 79.5071° W, 220 m above sea level). The HCl-TCl was co-located with a Campbell  
213 scientific weather station paired with a cr300 datalogger. All inlet lines and fittings were made of  
214 PFA unless stated otherwise. All indoor inlet lines and fittings were kept at room temperature (20  
215 to 25 °C) while outdoor temperatures ranged from 25 to 28 °C on August 6, and 0 to 17 °C in  
216 November. A mass flow controller (GM50A, MKS instruments, Andover, Massachusetts, USA)  
217 regulated a sampling flow of 14.7 L min<sup>-1</sup> using a diaphragm pump through a 2.4 m sampling  
218 inlet (I.D. of 0.375”) from outdoors. The outdoor air was pulled through a URG Teflon Coated  
219 Aluminum Cyclone (URG Corporation, Chapel Hill, North Carolina, USA) with a 2.5 µm  
220 particulate matter cut-off. The CRDS subsampled 2 L min<sup>-1</sup> through the furnace off the main  
221 inlet line, yielding a total inlet flow of 16.7 L min<sup>-1</sup>. The apparatus had zero air overflow the inlet  
222 1 hour prior to and after outdoor sampling. The CRDS sample flow passed first through a PTFE



223 filter (2  $\mu\text{m}$  pore size, 47 mm diameter, TISCH scientific, North Bend, Ohio, USA) and then two  
224 high efficiency particulate air (HEPA) filters contained within the CRDS outer cavity metal  
225 compartment heat-regulated to 45 °C. Instances of flagged instrument errors in the CRDS data  
226 during ambient observations were removed as standard practice in quality control procedures  
227 (Furlani et al., 2021).

## 228 **2.6. Indoor air HCl-TCl and HOCl analyzer measurements**

229 To test indoor applications of the HCl-TCl, a 1 m<sup>2</sup> area of laboratory floor was cleaned  
230 with a commercial spray bottle cleaner (1.84 % sodium hypochlorite w/w) and emissions were  
231 compared with an HOCl analyzer. The HOCl analyzer is a commercial instrument designed to  
232 quantify gaseous hydrogen peroxide (H<sub>2</sub>O<sub>2</sub>) using CRDS (Picarro PI2114 Hydrogen Peroxide  
233 Analyzer; Picarro Inc.). The instrument is also sensitive to HOCl due to similar absorbance  
234 wavelengths of their first overtone stretches in the near IR. The wavelengths monitored have  
235 been altered to selectively detect HOCl. Details on instrument calibration and validation are  
236 provided in [Stubbs et al., in prep].

237 The distance from the suspended 2 m inlet lines of both instruments to the floor was ~1 m.  
238 The flowrate through the furnace and inlet was the 2 L min<sup>-1</sup> CRDS flowrate. The flowrate for  
239 the HOCl analyzer was 1 L min<sup>-1</sup>. The sectioned off area was cleaned four times, spraying 32  
240 times for each application using the commercial cleaner. Three of these events were measured  
241 using the HCl-TCl and HOCl analyzer, while one event was measured using the HCl CRDS  
242 only.



### 243 3. Results and Discussion

#### 244 3.1. HCl-TCl temperature and residence time optimization

245 We validated this method by testing conversion efficiency of organochlorines under  
246 different operating parameters and conditions. Testing all TCl<sub>g</sub> species is not feasible, but by  
247 testing compounds that contain strong Cl-containing bonds, we infer at least equal efficacy of the  
248 system in the breakage of weaker Cl-containing bonds (Tables S1 and S2). We selected very  
249 strong Cl-containing bonds (i.e., alkyl chlorides) and used them as a proxy for compounds  
250 containing weaker Cl bonds; therefore, by demonstrating their complete conversion we set  
251 precedent for conversion of all TCl<sub>g</sub>. The temperature of the furnace is a key factor in  
252 accomplishing complete thermolysis, and the minimum temperature of the furnace containing the  
253 Pt catalyst to break the C-Cl bonds in DCM was determined. A simple temperature ramping  
254 program was used to determine the breakthrough temperature. The temperature was increased at  
255 a rate of 2.7 °C min<sup>-1</sup> starting at 300 °C and ending at 800 °C. The temperature breakthrough was  
256 found to be ~800 °C for the tested organochlorines (Figure S2).

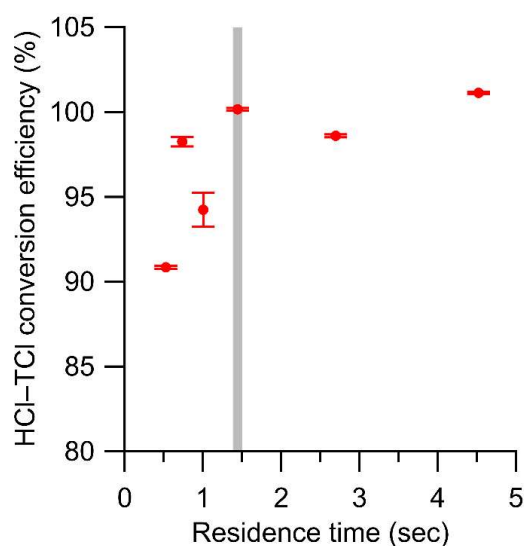
257 Determining the optimal residence time of sample gas in the HCl-TCl is also essential for  
258 an optimized TCl<sub>g</sub> conversion method. Using a temperature slightly above the observed  
259 breakthrough temperature of 800 °C determined above (825 °C), six residence times were tested  
260 with DCM, ranging from 0.5 to 4.5 seconds in the HCl-TCl (Figure 2). At each residence time  
261 the conversion efficiency was determined, where conversion efficiency was calculated as  
262 follows:

$$263 \text{ Conversion efficiency} = \frac{\text{Measured TCl}_g}{\text{Expected TCl}_g} \times 100 \% \quad \text{E1}$$

264 The optimal residence time was ~1.5 seconds, corresponding to a conversion efficiency of 100.1  
265 ± 0.1 %. The uncertainty in conversion efficiency measurements is the variability in the



266 measured HCl signal for 30 minutes after a signal plateau was observed. The reported  
267 uncertainty does not include uncertainties in mixing, or turbulence induced surface effects, which  
268 we cannot quantify. When residence times were lower (i.e., sample gas traveled more quickly  
269 through the system) than 1.5 seconds, the conversion efficiencies were lower by 2 – 10 %, the  
270 measured HCl signal was more erratic, and it took longer to stabilize. When residence times  
271 were higher (i.e., sample gas traveled more slowly through the system) than 1.5 seconds, the  
272 conversion efficiencies were comparable ( $\pm 2\%$ ), but the measured HCl suffered from longer  
273 equilibration times and therefore a slower response time due to increased surface effects of HCl  
274 after exiting the furnace. A residence time of 1.5 seconds was selected for all HCl-TCl  
275 experiments.



276

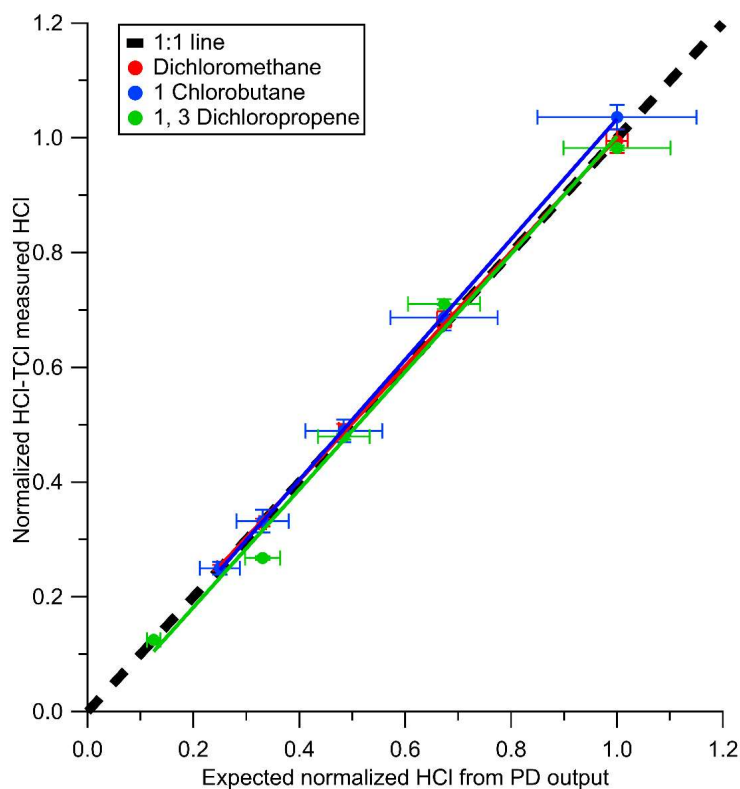
277 **Figure 2.** Conversion efficiency of DCM plotted against residence time in the HCl-TCl. Error  
278 bars represent the percent relative standard deviation of the measured HCl by the CRDS over  
279 ~30 minutes, after signal has plateaued. Grey vertical line denotes the selected residence time.

280



### 281 3.2. HCl-TCl conversion efficiency

282 The conversion efficiency of each of the three chosen organochlorines using the HCl-TCl  
283 was tested at 5 different mixing ratios. The mixing ratios tested for DCM were 41, 54, 80, 111,  
284 and 165 ppbv. The mixing ratios tested for CB were 3.5, 4.6, 6.8, 9.5, and 14 ppbv. The mixing  
285 ratios tested for DCP were 121, 259, 468, 651, and 967 ppbv. All three showed good linearity  
286 and near 1:1 correlation with the HCl expected to be formed from the PD under standard  
287 operating conditions (Figure 3). Due to differences in PD emission rates, the values in Figure 3  
288 are normalized to the highest mixing ratio to visualize comparisons more easily. Under condition  
289 (1) with both Pt and propane the HCl-TCl conversion was  $99.6 \pm 3.2$ ,  $104.8 \pm 5.6$ , and  $102.7 \pm$   
290  $7.8\%$  for DCM, CB, and DCP, respectively (Table 1). From Figure 3 the comparison between  
291 expected and measured  $\text{TCl}_g$  is illustrated by near unity in the orthogonal distance regression  
292 slope ( $\pm\sigma$ ), and was  $0.996 \pm 0.012$ ,  $1.048 \pm 0.006$ , and  $1.027 \pm 0.061$  for DCM, CB, and DCP,  
293 respectively. With only the Pt catalyst (condition (2)), the HCl-TCl conversion was  $80.7 \pm 0.4$ ,  
294  $54.1 \pm 1.6$ , and  $54.3 \pm 3.5\%$  for DCM, CB, and DCP, respectively (Figure S3, Table 1). This  
295 result indicates the added hydrogen source (propane) is needed to promote R1. Although  
296 necessary in this laboratory scenario, some ambient conditions may be rich enough hydrogen-  
297 containing molecules that excess propane is not needed. However, providing propane in excess  
298 ensures the presence of an abundance of hydrogen atoms that can be readily abstracted by Cl  
299 atoms via R1. When the Pt catalyst was removed (condition (3)) the HCl-TCl conversion was  
300  $94.4 \pm 4.6$ ,  $44.2 \pm 0.9$ , and  $41.7 \pm 3.4\%$  for DCM, CB, and DCP, respectively (Figure S3, Table  
301 1). The observed dependence of the Pt catalyst indicates that a reactive surface is important to  
302 achieve complete thermolysis at 825 °C. The relatively higher conversion for DCM in the  
303 absence of the Pt catalyst or hydrogen source may be attributed to its lower bond dissociation  
304 energy ( $310 \text{ kJ mol}^{-1}$ ) compared to estimated bond dissociation energies for CB and DCP (CB



305

306 **Figure 3.** HCl measured by CRDS plotted against the expected HCl from HCl-TCl converted  
 307 DCM (red), 1-chlorobutane (blue), and 1,3-dichloropropene (green) under condition (1). All  
 308 values are normalized to the highest expected HCl concentration to better illustrate deviations  
 309 from unity (dashed black line). Error bars on the y-axis represent  $1\sigma$  in the HCl signal over 10  
 310 minutes. Error bars on the x-axis represent the uncertainty in the PD used to generate DCM.

311 **Table 1.** Conversion efficiency for tested organochlorine compounds under the three conditions  
 312 (condition 1: both Pt and propane; condition 2: Pt only; condition 3: propane only). Conversion  
 313 efficiency was determined from the orthogonal distance regression slope and  $\pm \sigma$  and propagated  
 314 error from individual PDs.

Tested $\text{TCl}_g$ species	Bond dissociation energy ( $\text{kJ mol}^{-1}$ )	Conversion efficiency (%)		
		Condition 1	Condition 2	Condition 3
Dichloromethane	310	$99.6 \pm 3.2$	$80.7 \pm 2.4$	$94.4 \pm 6.6$
1-Chlorobutane	410	$104.8 \pm 5.6$	$54.1 \pm 6.6$	$44.2 \pm 5.9$
1, 3- Dichloropropene	350	$102.7 \pm 7.8$	$54.3 \pm 5.2$	$41.7 \pm 5.1$



315 inferred from Table S2 ( $\sim 410 \text{ kJ mol}^{-1}$ ), and DCP from tetrachloroethylene ( $350 \text{ kJ mol}^{-1}$  in  
316 Table S1)). It is possible that a higher temperature could lead to full conversion of  $\text{TCI}_g$  in the  
317 absence of Pt catalyst; however, that was not explored in this study. The results for all three  
318 compounds show that the HCl-TCl is capable of complete conversion of mono and  
319 polychlorinated species on  $\text{sp}^3$  and  $\text{sp}^2$  carbons using the determined temperature and flow  
320 conditions. The complete thermolysis of the strong C-Cl bond on the primary alkyl chloride (CB)  
321 demonstrates the efficacy of the HCl-TCl. Breaking these relatively strong C-Cl bonds is a good  
322 proof of concept for complete conversion of all bonds of similar or weaker bond energies that  
323 characterize all other  $\text{TCI}_g$ . To practically validate the HCl-TCl under real-world conditions with  
324 atmospherically relevant  $\text{TCI}_g$  mixtures and mixing ratios we deployed and configured the  
325 system to measure outdoor and indoor air.

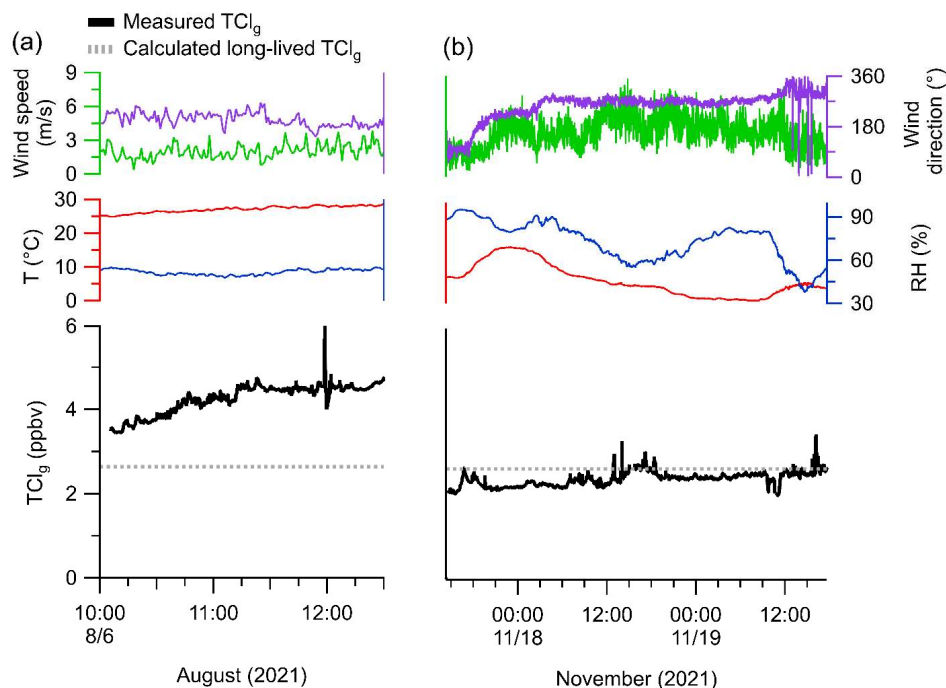
### 326 3.3. HCl-TCl applications to outdoor air

327 We deployed the system to measure ambient outdoor air, which we compare to the  
328 expected  $\text{TCI}_g$  range from complete thermolysis of total Cl, expected to be between 3.3 and 19  
329 ppbv (Table S1). A global background of approximately 2.6 ppbv is expected if only considering  
330 the controlled very long-lived species (WMO, 2018, Table S1). The effects of particulate  
331 chloride on  $\text{TCI}_g$  conversion were not explored here. The conditions required to convert chloride  
332 to chlorine atoms is typically achieved using high energy photons or by electron beams, which  
333 deliver energy much greater than possible in our system (Delahay, 1982; Kurepa and Belic,  
334 1978). Thus, chloride, if it enters the system, is assumed to not be converted and measured. The  
335 apparatus subsampled off a main inlet pulling ambient air (Figure 4) in summer (August 6) and  
336 winter (November 17–19). The maximum, minimum, and mean of observed  $\text{TCI}_g$  on August 6  
337 was 6.0, 3.4, and 4.2 ppbv, respectively, and was 3.5, 2.0, and 2.5 ppbv respectively from





338 November 17–19. Measurements of HCl alone were not made during these periods but reported  
339 ranges of HCl mixing ratios for this sampling location from Furlani et al. (2021) and Angelucci  
340 et al. (2021) are typically below 110 pptv, with intermittent events up to 600 pptv. Mixing ratios  
341 of TCl<sub>g</sub> were higher in the summer season when compared to the winter, suggesting a seasonal  
342 variance on the levels of TCl<sub>g</sub>. The mean August TCl<sub>g</sub> was 60% higher than the expected  
343 baseline of known long lived species. In contrast, levels of TCl<sub>g</sub> in the during the winter were  
344 near the expected global baseline. We generally observed higher TCl<sub>g</sub> during periods of lower  
345 relative humidity (RH), illustrated by the lower levels of TCl<sub>g</sub> and high RH observed during  
346 November. There was no observed impact on observed TCl<sub>g</sub> due to changes in wind direction or  
347 wind speed and likely indicates TCl<sub>g</sub> is relatively well mixed. Our observed seasonal differences  
348 in TCl<sub>g</sub> could have been caused, in part, by differences in meteorology (i.e., higher temperature  
349 in summer, higher relative humidity in winter) through changes in mixing and/or deposition.  
350 However, it seems likely that higher summer emissions, which have been observed for individual  
351 chlorinated species (Bin et al., 2014; Melymuk et al., 2012; Zhang et al., 2014) played an  
352 important role in the higher summertime TCl<sub>g</sub>. Rapid temporal changes in TCl<sub>g</sub> indicate the  
353 utility of an in-situ technique, which could be used to constrain sources and sinks of TCl<sub>g</sub>.



354

355 **Figure 4.** Monitoring meteorological conditions and  $\text{TCl}_g$  in outdoor air through HCl-TCl; (a)  
356 from 10 AM to 1 PM August 6, and (b) from 12 PM November 17 to 6 PM November 19. Grey  
357 dashed line represents the background mixing ratio for long-lived  $\text{TCl}_g$  species from Table S1.

### 358 3.4. HCl-TCl application to indoor cleaning

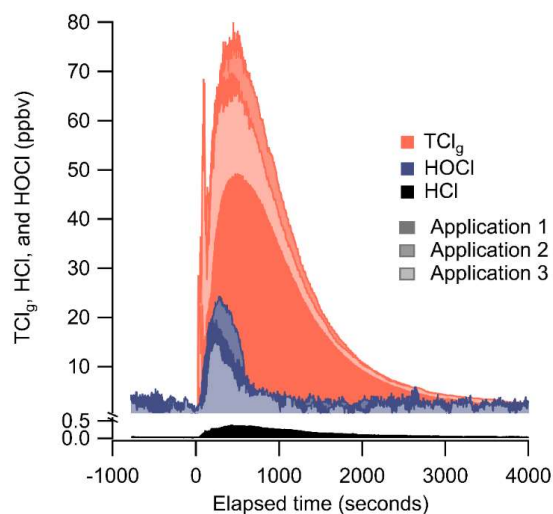
359 We applied a chlorine-based cleaning product four times in a well-lit indoor room and  
360 measured  $\text{TCl}_g$  using the HCl-TCl and HOCl analyzer during three of the cleaning events (Figure  
361 5). One cleaning experiment was done without the HCl-TCl and had a maximum of 370 pptv  
362 HCl. These levels are comparable to peak HCl levels of  $\sim 500$  pptv observed from surface  
363 application of bleach (Dawe et al., 2019). Consistent with previous speciated measurements  
364 (Mattila et al., 2020; Wong et al., 2017), HCl, HOCl, and  $\text{TCl}_g$  levels increased rapidly over  $\sim 5$   
365 minutes after the application of the cleaning product. The maximum levels of  $\text{TCl}_g$  from HCl-  
366 TCl during application 1, 2, and 3, were 49.2, 80.0, and 69.7 ppbv, respectively. The maximum  
367 levels of HOCl from applications 1, 2, and 3, were 19.6, 24.2, and 16.8 ppbv, respectively,



368 corresponding to 24 to 40 % of peak  $\text{TCI}_g$  and 14 to 22 % of integrated  $\text{TCI}_g$ . These  $\text{TCI}_g$  levels  
369 were several times higher than observed in outdoor air (Section 3.3) and were within the range  
370 expected from previous experiments (Table S1). The levels of chlorinated species observed  
371 during bleaching events is variable, between 15 to 100s of ppbv (Mattila et al., 2020; Odabasi,  
372 2008; Wang et al., 2019; Wong et al., 2017). By comparison, our highest observed mixing ratio  
373 was 80 ppbv. Because the multiphase chemical processes involved in bleach application are  
374 complex and poorly understood, it is difficult to compare levels between similar studies, given  
375 that the underlying ambient conditions can be very different. In addition, physical parameters,  
376 such as volume of cleaning solution applied, room size, and ventilation, can all affect observed  
377 mixing ratios. For example, studies have observed that gaseous  $\text{NH}_3$  partitioning into aqueous  
378 bleach can produce large and variable amounts of chloramines,  $\text{NH}_2\text{Cl}$ ,  $\text{NHCl}_2$ , and  $\text{NCl}_3$   
379 (Mattila et al., 2020; Wong et al., 2017). In our experiments, there was on average  $82 \pm 4$  % of  
380 integrated  $\text{TCI}_g$  for which we cannot account. Additional chlorinated species have previously  
381 been observed to be emitted from surface bleaching include  $\text{ClNO}_2$ ,  $\text{NH}_2\text{Cl}$ ,  $\text{NHCl}_2$ ,  $\text{NCl}_3$ , and  
382 several chlorinated organics (Mattila et al., 2020; Odabasi, 2008; Wong et al., 2017) which likely  
383 also contributed to our measured  $\text{TCI}_g$ . We observed that  $\text{TCI}_g$  decayed  $\sim 15\%$  faster than the air  
384 exchange rate ( $0.72 \text{ h}^{-1}$ ), indicating additional chemical loss pathways or surface interactions  
385 (Figure S4). We observed a shorter lifetime of  $\text{HOCl}$  relative to  $\text{TCI}_g$ , which is consistent with  
386 faster decay rates observed for  $\text{HOCl}$  and similar  $\text{TCI}_g$  species by Wong et al., (2017). The  
387  $\text{HOCl}$  started decreasing after  $\sim 300$  s had elapsed while the  $\text{TCI}_g$  levels were still increasing. This  
388 suggests that reactions involving  $\text{HOCl}$  may have led to additional  $\text{TCI}_g$  species, which has been  
389 observed in laboratory studies (Wang et al., 2019).



390 In-situ measurements of  $\text{TCI}_g$  could provide additional insight into sources of chlorinated  
391 species to indoor environments by creating a total inventory from which the contributions of  
392 individual measured species can be compared and used to elucidate unknown  $\text{TCI}_g$  levels and  
393 mechanisms in real-time. Furthermore, several chlorinated species that have previously been  
394 observed to be emitted from surface bleaching, including  $\text{Cl}_2$ ,  $\text{HOCl}$ ,  $\text{ClNO}_2$ ,  $\text{NH}_2\text{Cl}$ ,  $\text{NHCl}_2$ , and  
395  $\text{NCl}_3$  (Mattila et al., 2020; Wong et al., 2017), have been measured by chemical ionization mass  
396 spectrometry (CIMS). Quantifying chlorinated species using CIMS remains challenging due to  
397 the required calibrations and difficulty in generating pure gas phase standards. It is therefore  
398 desirable to have a technique such as the one proposed in this study that does not require  
399 calibrations or knowledge of potential unknown  $\text{TCI}_g$  species. A combination of the two methods  
400 would help constrain the total levels while still observing speciation for key  $\text{TCI}_g$  species.



401  
402 **Figure 5.** HCl (black), HOCl (dark blue), and  $\text{TCI}_g$  (orange) observed during cleaning spray  
403 events. Mixing ratios were background corrected prior to each cleaning event. Each subsequent  
404 application of cleaner is illustrated by a lighter shade for HOCl and  $\text{TCI}_g$ .



#### 405 **4. Conclusions**

406 In this work we developed, optimized, validated, and applied a method capable of  
407 converting  $\text{TCI}_g$  into gaseous HCl amenable for CRDS detection. Our  $\text{TCI}_g$  measurement  
408 technique, the HCl-TCl, is composed of a platinum catalyst mesh inside a quartz glass flow tube  
409 all contained within a split-tube furnace. The temperature and flow rate were optimized at 825 °C  
410 and 1.5 seconds, respectively using DCM. These conditions were validated by the complete  
411 conversion of organochlorine compounds with strong C-Cl bonds. The HCl-TCl was used to  
412 measure  $\text{TCI}_g$  outdoors, observing a range of 2.0–6.0 ppbv. Levels were comparable to (winter)  
413 or exceeded (summer) the calculated background mixing ratio of long-lived  $\text{TCI}_g$ . We also  
414 applied the HCl-TCl to an indoor environment during commercial bleach spray cleaning events  
415 and observed varying increases in  $\text{TCI}_g$  (50–80 ppbv), which was in reasonable agreement with  
416 levels observed in previous speciated measurements. The agreement of HCl-TCl outdoor and  
417 indoor measurements with available bottom-up estimates indicates its efficacy under real-world  
418 scenarios. Rapid changes in  $\text{TCI}_g$  were observed in both outdoor and indoor environments  
419 indicating the utility of an in-situ technique to constrain the sources and chemistry of  $\text{TCI}_g$ , as  
420 well as its impact on air quality, climate, and health. We anticipate this approach could be used  
421 in several applications, including comparisons to speciated measurements and to further explore  
422 Cl reactivity and cycling with respect for indoor and outdoor  $\text{TCI}_g$ .

#### 423 **Acknowledgements**

424 We acknowledge the Sloan Foundation, Natural Sciences Engineering and Research Council of  
425 Canada for funding. We thank Leigh Crilley, Melodie Lao, and Yashar Iranpour for collecting  
426 air exchange rate data and Dirk Verdoold for the custom quartz tube. PME thanks the European



427 Research Council. TFK is a Canada Research Chair in Environmental Analytical Chemistry.  
428 This work was undertaken, in part, thanks to funding from the Canada Research Chairs program.

#### 429 **Author contributions**

430 TCF collected and analyzed the data. TCF and CJY conceived of and designed the experiments  
431 with input from PME and TFK. Funding was obtained by TFK and CJY. The manuscript was  
432 written by TCF with input from all authors.

#### 433 **5. References**

- 434 Adcock, K. E., Reeves, C. E., Gooch, L. J., Leedham Elvidge, E. C., Ashfold, M. J.,  
435 Brenninkmeijer, C. A. M., Chou, C., Fraser, P. J., Langenfelds, R. L., Mohd Hanif, N.,  
436 O'Doherty, S., Oram, D. E., Ou-Yang, C.-F., Phang, S. M., Samah, A. A., Röckmann, T.,  
437 Sturges, W. T. and Laube, J. C.: Continued increase of CFC-113a (CCl<sub>3</sub>CF<sub>3</sub>) mixing ratios in  
438 the global atmosphere: emissions, occurrence and potential sources, *Atmos. Chem. Phys.*, 18(7),  
439 4737–4751, doi:10.5194/acp-18-4737-2018, 2018.
- 440 Andrews, S. J., Carpenter, L. J., Apel, E. C., Atlas, E., Donets, V., Hopkins, J. R., Hornbrook, R.  
441 S., Lewis, A. C., Lidster, R. T., Lueb, R., Minaeian, J., Navarro, M., Punjabi, S., Riemer, D. and  
442 Schauffler, S.: A comparison of very short lived halocarbon (VSLS) and DMS aircraft  
443 measurements in the tropical west Pacific from CAST, ATTREX and CONTRAST, *Atmos.*  
444 *Meas. Tech.*, 9(10), 5213–5225, doi:10.5194/amt-9-5213-2016, 2016.
- 445 Berg, W. W., Crutzen, P. J., Grahek, F. E., Gitlin, S. N. and Sedlacek, W. A.: First measurements  
446 of total chlorine and bromine in the lower stratosphere, *Geophys. Res. Lett.*, 7(11), 937–940,  
447 doi:https://doi.org/10.1029/GL007i011p00937, 1980.
- 448 Bin, X., K., P. P., A., M. S., M., M. S., W., E. J., L., M. F., L., A. E., R., M. Ben, F., W. R., G.,  
449 P. R. and C., W. S.: Global emissions of refrigerants HCFC-22 and HFC-134a: Unforeseen  
450 seasonal contributions, *Proc. Natl. Acad. Sci.*, 111(49), 17379–17384,  
451 doi:10.1073/pnas.1417372111, 2014.
- 452 Blankenship, A., Chang, D. P. Y., Jones, A. D., Kelly, P. B., Kennedy, I. M., Matsumura, F.,  
453 Pasek, R. and Yang, G.: Toxic combustion by-products from the incineration of chlorinated  
454 hydrocarbons and plastics, *Chemosphere*, 28(1), 183–196, doi:https://doi.org/10.1016/0045-  
455 6535(94)90212-7, 1994.
- 456 Butz, A., Dinger, A. S., Bobrowski, N., Kostinek, J., Fieber, L., Fischerkeller, C., Giuffrida, G.  
457 B., Hase, F., Klappenbach, F., Kuhn, J., Lübcke, P., Tirpitz, L. and Tu, Q.: Remote sensing of  
458 volcanic CO<sub>2</sub>, HF, HCl, SO<sub>2</sub>, and BrO in the downwind plume of Mt. Etna, *Atmos. Meas.*  
459 *Tech.*, 10(1), 1–14, doi:10.5194/amt-10-1-2017, 2017.
- 460 Dawe, K. E. R., Furlani, T. C., Kowal, S. F., Kahan, T. F., Vandenkoer, T. C. and Young, C. J.:  
461 Formation and emission of hydrogen chloride in indoor air, *Indoor Air*, (April 2018), 70–78,



- 462 doi:10.1111/ina.12509, 2019.
- 463 Delahay, P.: Photoelectron emission spectroscopy of aqueous solutions, *Acc. Chem. Res.*, 15(2),  
464 40–45, doi:10.1021/ar00074a002, 1982.
- 465 Doucette, W. J., Wetzel, T. A., Dettenmaier, E. and Gorder, K.: Emission rates of chlorinated  
466 volatile organics from new and used consumer products found during vapor intrusion  
467 investigations: Impact on indoor air concentrations, *Environ. Forensics*, 19(3), 185–190,  
468 doi:10.1080/15275922.2018.1475433, 2018.
- 469 Fernando, S., Jobst, K. J., Taguchi, V. Y., Helm, P. A., Reiner, E. J. and McCarry, B. E.:  
470 Identification of the Halogenated Compounds Resulting from the 1997 Plastimet Inc. Fire in  
471 Hamilton, Ontario, using Comprehensive Two-Dimensional Gas Chromatography and  
472 (Ultra)High Resolution Mass Spectrometry, *Environ. Sci. Technol.*, 48(18), 10656–10663,  
473 doi:10.1021/es503428j, 2014.
- 474 Finlayson-Pitts, B. J.: Chlorine Atoms as a Potential Tropospheric Oxidant in the Marine  
475 Boundary Layer, *Res. Chem. Intermed.*, 19(3), 235–249, doi:10.1163/156856793X00091, 1993.
- 476 Furlani, T. C., Veres, P. R., Dawe, K. E. R., Neuman, J. A., Brown, S. S., VandenBoer, T. C. and  
477 Young, C. J.: Validation of a new cavity ring-down spectrometer for measuring tropospheric  
478 gaseous hydrogen chloride, *Atmos. Meas. Tech. Discuss.*, 2021, 1–30, doi:10.5194/amt-2021-  
479 105, 2021.
- 480 Giardino, N. J. and Andelman, J. B.: Characterization of the emissions of trichloroethylene,  
481 chloroform, and 1,2-dibromo-3-chloropropane in a full-size, experimental shower., *J. Expo.*  
482 *Anal. Environ. Epidemiol.*, 6(4), 413–423, 1996.
- 483 Hardy, J. E. and Knarr, J. J.: Technique for Measuring the Total Concentration of Gaseous Fixed  
484 Nitrogen Species, *J. Air Pollut. Control Assoc.*, 32(4), 376–379,  
485 doi:10.1080/00022470.1982.10465412, 1982.
- 486 Haskins, J. D., Jaeglé, L., Shah, V., Lee, B. H., Lopez-Hilfiker, F. D., Campuzano-Jost, P.,  
487 Schroder, J. C., Day, D. A., Guo, H., Sullivan, A. P., Weber, R., Dibb, J., Campos, T., Jimenez,  
488 J. L., Brown, S. S. and Thornton, J. A.: Wintertime Gas-Particle Partitioning and Speciation of  
489 Inorganic Chlorine in the Lower Troposphere Over the Northeast United States and Coastal  
490 Ocean, *J. Geophys. Res. Atmos.*, 123(22), 12,812–897,916, doi:10.1029/2018JD028786, 2018.
- 491 Henschler, D.: Toxicity of Chlorinated Organic Compounds: Effects of the Introduction of  
492 Chlorine in Organic Molecules, *Angew. Chemie Int. Ed. English*, 33(19), 1920–1935,  
493 doi:https://doi.org/10.1002/anie.199419201, 1994.
- 494 Kannan, K., Kawano, M., Kashima, Y., Matsui, M. and Giesy, J. P.: Extractable Organohalogen  
495 (EOX) in Sediment and Biota Collected at an Estuarine Marsh near a Former Chloralkali  
496 Facility, *Environ. Sci. Technol.*, 33(7), 1004–1008, doi:10.1021/es9811142, 1999.
- 497 Kato, M., Urano, K. and Tasaki, T.: Development of Semi- and Nonvolatile Organic Halogen as  
498 a New Hazardous Index of Flue Gas, *Environ. Sci. Technol.*, 34(19), 4071–4075,  
499 doi:10.1021/es000881+, 2000.
- 500 Kawano, M., Falandysz, J. and Wakimoto, T.: Instrumental neutron activation analysis of  
501 extractable organohalogenes in the Antarctic Weddell seal (*Leptonychotes weddelli*), *J.*





- 502 Radioanal. Nucl. Chem., 272(3), 501–504, doi:10.1007/s10967-007-0611-5, 2007.
- 503 Keene, W. C., Khalil, M. A. K., Erickson, D. J., McCulloch, A., Graedel, T. E., Lobert, J. M.,  
504 Aucott, M. L., Gong, S. L., Harper, D. B., Kleiman, G., Midgley, P., Moore, R. M., Seuzaret, C.,  
505 Sturges, W. T., Benkovitz, C. M., Koropalov, V., Barrie, L. A. and Li, Y. F.: Composite global  
506 emissions of reactive chlorine from anthropogenic and natural sources: Reactive Chlorine  
507 Emissions Inventory, *J. Geophys. Res. Atmos.*, 104(D7), 8429–8440,  
508 doi:10.1029/1998JD100084, 1999.
- 509 Khalil, M. A. K., Moore, R. M., Harper, D. B., Lobert, J. M., Erickson, D. J., Koropalov, V.,  
510 Sturges, W. T. and Keene, W. C.: Natural emissions of chlorine-containing gases: Reactive  
511 Chlorine Emissions Inventory, *J. Geophys. Res. Atmos.*, 104(D7), 8333–8346,  
512 doi:10.1029/1998JD100079, 1999.
- 513 Kurepa, M. V and Belic, D. S.: Electron-chlorine molecule total ionisation and electron  
514 attachment cross sections, *J. Phys. B At. Mol. Phys.*, 11(21), 3719–3729, doi:10.1088/0022-  
515 3700/11/21/017, 1978.
- 516 Lao, M., Crilley, L. R., Salehpoor, L., Furlani, T. C., Bourgeois, I., Neuman, J. A., Rollins, A.  
517 W., Veres, P. R., Washenfelder, R. A., Womack, C. C., Young, C. J. and VandenBoer, T. C.: A  
518 portable, robust, stable and tunable calibration source for gas-phase nitrous acid (HONO),  
519 *Atmos. Meas. Tech.*, 13, 5873–5890, doi:10.5194/amt-13-5873-2020, 2020.
- 520 Lobert, J. M., Keene, W. C., Logan, J. A. and Yevich, R.: Global chlorine emissions from  
521 biomass burning: Reactive Chlorine Emissions Inventory, *J. Geophys. Res. Atmos.*, 104(D7),  
522 8373–8389, doi:10.1029/1998JD100077, 1999.
- 523 Maris, C., Chung, M. Y., Lueb, R., Krischke, U., Meller, R., Fox, M. J. and Paulson, S. E.:  
524 Development of instrumentation for simultaneous analysis of total non-methane organic carbon  
525 and volatile organic compounds in ambient air, *Atmos. Environ.*, 37, 149–158,  
526 doi:https://doi.org/10.1016/S1352-2310(03)00387-X, 2003.
- 527 Massin, N., Bohadana, A. B., Wild, P., Héry, M., Toamain, J. P. and Hubert, G.: Respiratory  
528 symptoms and bronchial responsiveness in lifeguards exposed to nitrogen trichloride in indoor  
529 swimming pools., *Occup. Environ. Med.*, 55(4), 258 LP – 263, doi:10.1136/oem.55.4.258, 1998.
- 530 Mattila, J. M., Lakey, P. S. J., Shiraiwa, M., Wang, C., Abbatt, J. P. D., Arata, C., Goldstein, A.  
531 H., Ampollini, L., Katz, E. F., DeCarlo, P. F., Zhou, S., Kahan, T. F., Cardoso-Saldaña, F. J.,  
532 Ruiz, L. H., Abeleira, A., Boedicker, E. K., Vance, M. E. and Farmer, D. K.: Multiphase  
533 Chemistry Controls Inorganic Chlorinated and Nitrogenated Compounds in Indoor Air during  
534 Bleach Cleaning, *Environ. Sci. Technol.*, 54(3), 1730–1739, doi:10.1021/acs.est.9b05767, 2020.
- 535 Melymuk, L., Robson, M., Helm, P. A. and Diamond, M. L.: PCBs, PBDEs, and PAHs in  
536 Toronto air: Spatial and seasonal trends and implications for contaminant transport, *Sci. Total  
537 Environ.*, 429, 272–280, doi:https://doi.org/10.1016/j.scitotenv.2012.04.022, 2012.
- 538 Miyake, Y., Kato, M. and Urano, K.: A method for measuring semi- and non-volatile organic  
539 halogens by combustion ion chromatography, *J. Chromatogr. A*, 1139(1), 63–69,  
540 doi:https://doi.org/10.1016/j.chroma.2006.10.078, 2007a.
- 541 Miyake, Y., Yamashita, N., Rostkowski, P., So, M. K., Taniyasu, S., Lam, P. K. S. and Kannan,





- 542 K.: Determination of trace levels of total fluorine in water using combustion ion chromatography  
543 for fluorine: A mass balance approach to determine individual perfluorinated chemicals in water,  
544 *J. Chromatogr. A*, 1143(1), 98–104, doi:https://doi.org/10.1016/j.chroma.2006.12.071, 2007b.
- 545 Miyake, Y., Yamashita, N., So, M. K., Rostkowski, P., Taniyasu, S., Lam, P. K. S. and Kannan,  
546 K.: Trace analysis of total fluorine in human blood using combustion ion chromatography for  
547 fluorine: A mass balance approach for the determination of known and unknown organofluorine  
548 compounds, *J. Chromatogr. A*, 1154(1), 214–221,  
549 doi:https://doi.org/10.1016/j.chroma.2007.03.084, 2007c.
- 550 Montzka, S. A., Dutton, G. S., Portmann, R. W., Chipperfield, M. P., Davis, S., Feng, W.,  
551 Manning, A. J., Ray, E., Rigby, M., Hall, B. D., Siso, C., Nance, J. D., Krummel, P. B., Mühle,  
552 J., Young, D., O’Doherty, S., Salameh, P. K., Harth, C. M., Prinn, R. G., Weiss, R. F., Elkins, J.  
553 W., Walter-Terrinoni, H. and Theodoridi, C.: A decline in global CFC-11 emissions during  
554 2018–2019, *Nature*, 590(7846), 428–432, doi:10.1038/s41586-021-03260-5, 2021.
- 555 Nuckols, J. R., Ashley, D. L., Lyu, C., Gordon, S. M., Hinckley, A. F. and Singer, P.: Influence  
556 of tap water quality and household water use activities on indoor air and internal dose levels of  
557 trihalomethanes, *Environ. Health Perspect.*, 113(7), 863–870, doi:10.1289/ehp.7141, 2005.
- 558 Odabasi, M.: Halogenated Volatile Organic Compounds from the Use of Chlorine-Bleach-  
559 Containing Household Products, *Environ. Sci. Technol.*, 42(5), 1445–1451,  
560 doi:10.1021/es702355u, 2008.
- 561 Odabasi, M., Elbir, T., Dumanoglu, Y. and Sofuoglu, S.: Halogenated volatile organic  
562 compounds in chlorine-bleach-containing household products and implications for their use,  
563 *Atmos. Environ.*, 92, 376–383, doi:10.1016/j.atmosenv.2014.04.049, 2014.
- 564 Pan, L. L., Atlas, E. L., Salawitch, R. J., Honomichl, S. B., Bresch, J. F., Randel, W. J., Apel, E.  
565 C., Hornbrook, R. S., Weinheimer, A. J., Anderson, D. C., Andrews, S. J., Baidar, S., Beaton, S.  
566 P., Campos, T. L., Carpenter, L. J., Chen, D., Dix, B., Donets, V., Hall, S. R., Hanisco, T. F.,  
567 Homeyer, C. R., Huey, L. G., Jensen, J. B., Kaser, L., Kinnison, D. E., Koenig, T. K., Lamarque,  
568 J.-F., Liu, C., Luo, J., Luo, Z. J., Montzka, D. D., Nicely, J. M., Pierce, R. B., Riemer, D. D.,  
569 Robinson, T., Romashkin, P., Saiz-Lopez, A., Schauffler, S., Shieh, O., Stell, M. H., Ullmann,  
570 K., Vaughan, G., Volkamer, R. and Wolfe, G.: The Convective Transport of Active Species in  
571 the Tropics (CONTRAST) Experiment, *Bull. Am. Meteorol. Soc.*, 98(1), 106–128,  
572 doi:10.1175/BAMS-D-14-00272.1, 2017.
- 573 Prinn, R. G., Weiss, R. F., Arduini, J., Arnold, T., DeWitt, H. L., Fraser, P. J., Ganesan, A. L.,  
574 Gasore, J., Harth, C. M., Hermansen, O., Kim, J., Krummel, P. B., Li, S., Loh, Z. M., Lunder, C.  
575 R., Maione, M., Manning, A. J., Miller, B. R., Mitrevski, B., Mühle, J., O’Doherty, S., Park, S.,  
576 Reimann, S., Rigby, M., Saito, T., Salameh, P. K., Schmidt, R., Simmonds, P. G., Steele, L. P.,  
577 Vollmer, M. K., Wang, R. H., Yao, B., Yokouchi, Y., Young, D. and Zhou, L.: History of  
578 chemically and radiatively important atmospheric gases from the Advanced Global Atmospheric  
579 Gases Experiment (AGAGE), *Earth Syst. Sci. Data*, 10(2), 985–1018, doi:10.5194/essd-10-985-  
580 2018, 2018.
- 581 Raff, J. D., Njegic, B., Chang, W. L., Gordon, M. S., Dabdub, D., Gerber, R. B. and Finlayson-  
582 Pitts, B. J.: Chlorine activation indoors and outdoors via surface-mediated reactions of nitrogen  
583 oxides with hydrogen chloride, *Proc. Natl. Acad. Sci.*, 106(33), 13647 LP – 13654,



- 584 doi:10.1073/pnas.0904195106, 2009.
- 585 Riedel, T. P., Wolfe, G. M., Danas, K. T., Gilman, J. B., Kuster, W. C., Bon, D. M., Vlasenko,  
586 A., Li, S.-M., Williams, E. J., Lerner, B. M., Veres, P. R., Roberts, J. M., Holloway, J. S., Lefer,  
587 B., Brown, S. S. and Thornton, J. A.: An MCM modeling study of nitryl chloride (ClNO<sub>2</sub>)  
588 impacts on oxidation, ozone production and nitrogen oxide partitioning in polluted continental  
589 outflow, *Atmos. Chem. Phys.*, 14(8), 3789–3800, doi:10.5194/acp-14-3789-2014, 2014.
- 590 Roberts, J. M., Bertman, S. B., Jobson, T., Niki, H. and Tanner, R.: Measurement of total  
591 nonmethane organic carbon (Cy): Development and application at Chebogue Point, Nova Scotia,  
592 during the 1993 North Atlantic Regional Experiment campaign, *J. Geophys. Res. Atmos.*,  
593 103(D11), 13581–13592, doi:https://doi.org/10.1029/97JD02240, 1998.
- 594 Saiz-Lopez, A. and Von Glasow, R.: Reactive halogen chemistry in the troposphere, *Chem. Soc.*  
595 *Rev.*, 41(19), 6448–6472, doi:10.1039/c2cs35208g, 2012.
- 596 Schwartz-Narbonne, H., Wang, C., Zhou, S., Abbatt, J. P. D. and Faust, J.: Heterogeneous  
597 Chlorination of Squalene and Oleic Acid, *Environ. Sci. Technol.*, 53(3), 1217–1224,  
598 doi:10.1021/acs.est.8b04248, 2019.
- 599 Shepherd, J. L., Corsi, R. L. and Kemp, J.: Chloroform in Indoor Air and Wastewater: The Role  
600 of Residential Washing Machines., *J. Air Waste Manag. Assoc.*, 46(7), 631–642,  
601 doi:10.1080/10473289.1996.10467497, 1996.
- 602 Sherwen, T., Schmidt, J. A., Evans, M. J., Carpenter, L. J., Großmann, K., Eastham, S. D., Jacob,  
603 D. J., Dix, B., Koenig, T. K., Sinreich, R., Ortega, I., Volkamer, R., Saiz-Lopez, A., Prados-  
604 Roman, C., Mahajan, A. S. and Ordóñez, C.: Global impacts of tropospheric halogens (Cl, Br, I)  
605 on oxidants and composition in GEOS-Chem, *Atmos. Chem. Phys.*, 16(18), 12239–12271,  
606 doi:10.5194/acp-16-12239-2016, 2016.
- 607 Simpson, W. R., Brown, S. S., Saiz-Lopez, A., Thornton, J. A. and Von Glasow, R.:  
608 Tropospheric Halogen Chemistry: Sources, Cycling, and Impacts, *Chem. Rev.*, 115(10), 4035–  
609 4062, doi:10.1021/cr5006638, 2015.
- 610 Solomon, S.: Stratospheric ozone depletion: A review of concepts and history, *Rev. Geophys.*,  
611 37(3), 275–316, doi:10.1029/1999RG900008, 1999.
- 612 Stockwell, C. E., Kupc, A., Witkowski, B., Talukdar, R. K., Liu, Y., Selimovic, V., Zarzana, K.  
613 J., Sekimoto, K., Warneke, C., Washenfelder, R. A., Yokelson, R. J., Middlebrook, A. M. and  
614 Roberts, J. M.: Characterization of a catalyst-based conversion technique to measure total  
615 particulate nitrogen and organic carbon and comparison to a particle mass measurement  
616 instrument, *Atmos. Meas. Tech.*, 11(5), 2749–2768, doi:10.5194/amt-11-2749-2018, 2018.
- 617 Unsal, V., Cicek, M. and Sabancilar, İ.: Toxicity of carbon tetrachloride, free radicals and role of  
618 antioxidants, *Rev. Environ. Health*, 36(2), 279–295, doi:doi:10.1515/reveh-2020-0048, 2021.
- 619 Veres, P., Gilman, J. B., Roberts, J. M., Kuster, W. C., Warneke, C., Burling, I. R. and de Gouw,  
620 J.: Development and validation of a portable gas phase standard generation and calibration  
621 system for volatile organic compounds, *Atmos. Meas. Tech.*, 3(3), 683–691, doi:10.5194/amt-3-  
622 683-2010, 2010.
- 623 Wang, C., Collins, D. B. and Abbatt, J. P. D.: Indoor Illumination of Terpenes and Bleach



- 624 Emissions Leads to Particle Formation and Growth, *Environ. Sci. Technol.*, 53(20), 11792–  
625 11800, doi:10.1021/acs.est.9b04261, 2019.
- 626 White, C. W. and Martin, J. G.: Chlorine Gas Inhalation, *Proc. Am. Thorac. Soc.*, 7(4), 257–263,  
627 doi:10.1513/pats.201001-008SM, 2010.
- 628 WMO (World Meteorological Organization), Scientific Assessment of Ozone Depletion: 2018,  
629 Global Ozone Research and Monitoring Project – Report No. 58, 588 pp., Geneva, Switzerland,  
630 2018.
- 631 Wong, J. P. S., Carslaw, N., Zhao, R., Zhou, S. and Abbatt, J. P. D.: Observations and impacts of  
632 bleach washing on indoor chlorine chemistry, *Indoor Air*, 27(6), 1082–1090,  
633 doi:10.1111/ina.12402, 2017.
- 634 Xu, D., Zhong, W., Deng, L., Chai, Z. and Mao, X.: Levels of Extractable Organohalogens in  
635 Pine Needles in China, *Environ. Sci. Technol.*, 37(1), 1–6, doi:10.1021/es025799o, 2003.
- 636 Xu, D., Tian, Q. and Chai, Z.: Determination of extractable organohalogens in the atmosphere by  
637 instrumental neutron activation analysis, *J. Radioanal. Nucl. Chem.*, 270(1), 5–8,  
638 doi:10.1007/s10967-006-0302-7, 2006.
- 639 Xu, D., Dan, M., Song, Y., Chai, Z. and Zhuang, G.: Instrumental neutron activation analysis of  
640 extractable organohalogens in PM<sub>2.5</sub> and PM<sub>10</sub> in Beijing, China, *J. Radioanal. Nucl. Chem.*,  
641 271(1), 115–118, doi:10.1007/s10967-007-0115-3, 2007.
- 642 Yeung, L. W. Y., Miyake, Y., Taniyasu, S., Wang, Y., Yu, H., So, M. K., Jiang, G., Wu, Y., Li,  
643 J., Giesy, J. P., Yamashita, N. and Lam, P. K. S.: Perfluorinated Compounds and Total and  
644 Extractable Organic Fluorine in Human Blood Samples from China, *Environ. Sci. Technol.*,  
645 42(21), 8140–8145, doi:10.1021/es800631n, 2008.
- 646 Young, C. J., Washenfelder, R. A., Edwards, P. M., Parrish, D. D., Gilman, J. B., Kuster, W. C.,  
647 Mielke, L. H., Osthoff, H. D., Tsai, C., Pikelnaya, O., Stutz, J., Veres, P. R., Roberts, J. M.,  
648 Griffith, S., Dusanter, S., Stevens, P. S., Flynn, J., Grossberg, N., Lefer, B., Holloway, J. S.,  
649 Peischl, J., Ryerson, T. B., Atlas, E. L., Blake, D. R. and Brown, S. S.: Chlorine as a primary  
650 radical: Evaluation of methods to understand its role in initiation of oxidative cycles, *Atmos.*  
651 *Chem. Phys.*, 14(7), 3427–3440, doi:10.5194/acp-14-3427-2014, 2014.
- 652 Zhai, S., Wang, X., McConnell, J. R., Geng, L., Cole-Dai, J., Sigl, M., Chellman, N., Sherwen,  
653 T., Pound, R., Fujita, K., Hattori, S., Moch, J. M., Zhu, L., Evans, M., Legrand, M., Liu, P.,  
654 Pasteris, D., Chan, Y.-C., Murray, L. T. and Alexander, B.: Anthropogenic Impacts on  
655 Tropospheric Reactive Chlorine Since the Preindustrial, *Geophys. Res. Lett.*, 48(14),  
656 e2021GL093808, doi:https://doi.org/10.1029/2021GL093808, 2021.
- 657 Zhang, G., Mu, Y., Liu, J., Zhang, C., Zhang, Y., Zhang, Y. and Zhang, H.: Seasonal and diurnal  
658 variations of atmospheric peroxyacetyl nitrate, peroxypropionyl nitrate, and carbon tetrachloride  
659 in Beijing, *J. Environ. Sci.*, 26(1), 65–74, doi:https://doi.org/10.1016/S1001-0742(13)60382-4,  
660 2014.
- 661 Zhang, W., Jiao, Y., Zhu, R., Rhew, R. C., Sun, B. and Dai, H.: Chloroform (CHCl<sub>3</sub>) Emissions  
662 From Coastal Antarctic Tundra, *Geophys. Res. Lett.*, 48(18), e2021GL093811,  
663 doi:https://doi.org/10.1029/2021GL093811, 2021.